Available online at www.sciencedirect.com
SCIENCE DIRECT®
Journal of Chromatography A, 1017 (2003) 45–61
JOURNAL OF CHROMATOGRAPHY A
www.elsevier.com/locate/chroma

Overloaded gradient elution chromatography on heterogeneous adsorbents in reversed-phase liquid chromatography

Fabrice Gritti[a,b], Attila Felinger[a,b], Georges Guiochon[a,b,*]

[a] *Department of Chemistry, University of Tennessee, Knoxville, TN 37996-1600, USA*
[b] *Division of Chemical Sciences, Oak Ridge National Laboratory, Oak Ridge, TN 37831-6120, USA*

Received 26 May 2003; received in revised form 15 July 2003; accepted 16 July 2003

Abstract

Overloaded band profiles of phenol were measured on a C_{18}-Kromasil column in gradient elution conditions. The mobile phase used was a mixture of methanol and water. The volume fraction of methanol was allowed to vary between 0 and 0.5. A general adsorption model, which expresses the amount of phenol adsorbed q^* as a function of both its concentration C and the composition φ of the organic modifier (methanol) in the mobile phase, was empirically derived from previous independent adsorption experiments based on frontal analysis (FA) and frontal analysis by the characteristic point (FACP). Accordingly, the general model was an extension of the simplest heterogeneous model, the Bilangmuir model, to non-isocratic conditions. The low-energy sites followed the classical linear solvent strength model (LSSM), but not the high-energy sites whose saturation capacity linearly decreased with φ. The general model was validated by comparing the experimental and simulated band profiles in gradient elution conditions, in linear and non-linear conditions, as well. The band profiles were calculated by means of the equilibrium-dispersive model of chromatography with a finite difference algorithm. A very good agreement was observed using steps gradient ($\Delta\varphi$) from 0 to 50% methanol and gradient times t_g of 20, 25, 30, 40, 60, 80 and 100 min. The agreement was still excellent for steps gradient from 5 to 45% ($t_g = 25$ min), 5 to 35% ($t_g = 50$ min), 5 to 25% ($t_g = 50$ min) and 5 to 15% ($t_g = 50$ min). Significative differences appeared between experience and simulation when the slope of the gradient ($\Delta\varphi/t_g$) became too strong beyond 3.3% methanol per minute. This threshold value probably mirrored the kinetic of arrangement of the G_{18}-bonded chains when the methanol content increased in the mobile phase. It suggested that the chromatographic system was not in a full thermodynamic equilibrium state when very steep mobile phase gradients were applied.

Keywords: Stationary phases, LC; Overloaded band profiles; Heterogeneous surface; General isotherm modeling; Gradient elution; Preparative chromatography; Phenol

1. Introduction

The accurate modeling of band profiles in chromatography requires a priori fundamental knowledge of the thermodynamics and kinetics of the phase equilibrium involved in the separation studied [1–3]. When

* Corresponding author. Tel.: +1-865-974-0733; fax: +1-865-974-2667.
E-mail address: guiochon@utk.edu (G. Guiochon).

0021-9673/$ – see front matter © 2003 Elsevier B.V. All rights reserved.
doi:10.1016/S0021-9673(03)01285-8

the solute mass transfer between the stationary and the mobile phases across the column is not too slow, elution band profiles are largely controlled by the thermodynamics of phase equilibrium. So, for single component bands, the relationship between the amount of solute adsorbed on the stationary phase and its concentration in the mobile phase must be known. For the separation of mixtures, the competitive isotherms of their components are necessary. Knowledge of these isotherms is required in the whole range of composition of the mobile phase used in the separation. Numerous models of adsorption isotherms are available to account for these adsorption data [1]. The modeling of band profiles [3] and the optimization of preparative separations [4–6] have largely been studied under isocratic conditions.

However, preparative separations are sometimes performed in displacement or gradient elution chromatography. Although, for reasons related to the difficulties and cost of the recycling of the mobile phase, this mode is less favored than the isocratic one for industrial separations, it would be useful to have solid information comparing the performance of gradient and isocratic elution chromatography for some typical separations. This work could be used as the technical basis of sound economical calculations. Attempts have been made to calculate the elution profiles of high-concentration bands in gradient elution [7–9]. The prediction of experimental band profiles under gradient elution conditions was investigated by El Fallah and Guiochon for low molecular-mass compounds [10,11] and for moderate molecular-mass biomolecules [12]. Recent works have investigated the optimization by numerical methods of preparative separations in overloaded gradient elution chromatography [13] and compared the optimum performance of the different modes of preparative liquid chromatography (elution, gradient and displacement) [14].

For the sake of simplicity, these studies have assumed that the Linear Solvent Strength Model (LSSM) applies to the description of the variation of the Henry constant with the organic modifier fraction (φ). Also, a simple Langmuir isotherm model is most often considered in theoretical studies to describe the solute adsorption. Accordingly, the saturation capacities of all the components are assumed to be equal (to achieve thermodynamical consistency of the competitive Langmuir isotherms) and are kept constant over the gradient range (LSSM). The former assumption is often reasonable for the separation of closely related compounds which are structurally similar. The latter one is probably valid as long as the amplitude of the gradient remains small, as is the case for gradient elution chromatography of proteins like lysozyme [12]. As the retention of proteins decreases extremely fast with increasing organic content of the mobile phase, the range of mobile phase composition experienced in their gradient elution is quite narrow.

However, these approximations are incorrect in many practical cases. Then, profile modeling based on these assumptions would fail. We recently derived a general isotherm model for phenol in water–methanol solutions [15]. We demonstrated that the adsorption of phenol on classical RPLC columns, from solutions of methanol and water ($\varphi = 0\%$ [15], $\varphi = 30$ to 60% [16]) [17] is controlled by the coexistence of two types of adsorption sites. The low-energy sites follow accurately the LSSM and their saturation capacity is practically independent of φ. In other words, the Henry constant of these sites is essentially governed by the solubility of phenol in the mobile phase. As for the high-energy sites, their Henry constant depends in both the solubility of phenol in the mobile phase and the number of these sites which increases with decreasing φ. We showed that this increase of the number of high-energy adsorption sites is probably related to the formation of new sites within the C_{18} bonded layer at low methanol content rather than with the liberation of sites occupied by methanol, i.e. with the competition for adsorption between methanol and phenol [15]. Such a competition is improbable because of the very weak adsorption of methanol on the C_{18}-Kromasil column in pure water.

In this work, we investigate the use of our general isotherm model [15] and show how the agreement between calculated and experimental band profiles validates it. We measured various overloaded band profiles in gradient elution chromatography and compare them to those calculated by means of the equilibrium-dispersive model of chromatography [1,3]. Finally, we discuss the validity of the model under linear conditions and the effect of the slope of the gradient on the agreement between experience and calculation results.

2. Theory

2.1. General model of isotherm for gradient elution

The model used to describe the general adsorption of phenol on a C_{18}-Kromasil column was derived from previous adsorption results [16,17]. Adsorption data were acquired by FA using various solutions of water and methanol, with a methanol volume fraction, φ, between 0.30 and 0.60 and by FACP in pure water ($\varphi = 0$). According to these two independent sets of results, the following empirical model was derived (see Fig. 1).

$$q^*(C,\varphi) = q_{1,0}\frac{b_{1,0}\exp(-S_{b_1}\varphi)C}{1+b_{1,0}\exp(-S_{b_1}\varphi)C} + (q_{2,0}-S_{q_2}\varphi)\frac{b_{2,0}\exp(-S_{b_2}\varphi)C}{1+b_{2,0}\exp(-S_{b_2}\varphi)C} \quad (1)$$

where the subscripts 1 and 2 refer to the low- and high-energy sites, respectively, $q_{1,0}$ is a constant, $b_{1,0}$ and S_{b_1} are the intercept and the slope of the plot of $\ln(b_1)$ versus the methanol fraction, φ, respectively, $q_{2,0}$ and S_{q_2} are the intercept and the slope of the plot of $q_{S,2}$ versus φ, respectively, and $b_{2,0}$ and S_{b_2} are the intercept and the slope of the plot of $\ln(b_2)$ versus φ, respectively. The best values of the numerical parameters of this general isotherm are given in Table 1.

This empirical model is based on the Bilangmuir model which was shown to be the model that accounts best for the adsorption isotherm data of phenol in equilibrium with methanol–water solutions on the RPLC Kromasil column. It is the simplest model for a non-homogeneous surface, which it assumed to be paved with only two types of homogeneous chemical domains, behaving independently [18]. Two further remarks must be made: (1) the low-energy sites follow the LSSM (their saturation capacity, $q_{S,1}$, is independent of φ); and (2) the saturation capacity of the high-energy sites, $q_{S,2}$, depends strongly on the mobile phase composition, it increases linearly with decreasing φ.

Table 1
Best empirical parameters coefficients of the general adsorption isotherm

$q_{1,0}$	123.3 g/l
$b_{1,0}$	0.0464 l/g
S_{b_1}	2.840
$q_{2,0}$	111.3 g/l
S_{q_2}	171.7 g/l
$b_{2,0}$	0.5753 l/g
S_{b_2}	4.558

2.2. Modeling of band profiles in overloaded gradient elution chromatography

The overloaded band profiles recorded under various experimental conditions were compared with profiles calculated using the general isotherm described earlier and the equilibrium-dispersive model (ED) of chromatography [1,3,19,20]. The ED model assumes instantaneous equilibrium between the mobile and the stationary phases and a finite column efficiency originating from an apparent axial dispersion coefficient, D_a, that accounts for the dispersive phenomena (molecular and eddy diffusion) and for the non-equilibrium effects that take place in a chromatographic column. The axial dispersion coefficient is:

$$D_a = \frac{uL}{2N} \quad (2)$$

where u is the mobile phase linear velocity, L the column length, and N the number of theoretical plates or apparent efficiency of the column.

In this model, the mass balance equation for a single component is written:

$$\frac{\partial C}{\partial t} + u\frac{\partial C}{\partial z} + F\frac{\partial q^*}{\partial t} = D_a\frac{\partial^2 C}{\partial z^2} \quad (3)$$

where q^* and C are the stationary and the mobile phase concentrations of the adsorbate, respectively, t is the time, z the distance along the column, and $F = (1-\varepsilon_t)/\varepsilon_t$ is the local phase ratio, with ε_t the total column porosity at time t and distance z. q^* is related to C through the isotherm equation, $q^* = f(C)$. Eq. (3) is a local equation, valid everywhere in the column.

2.2.1. Numerical solutions of the ED model

The mass balance equation was integrated numerically using a finite difference method [13,21]. The algorithm replaces the right hand side of the mass balance equation (dispersion term) with zero,

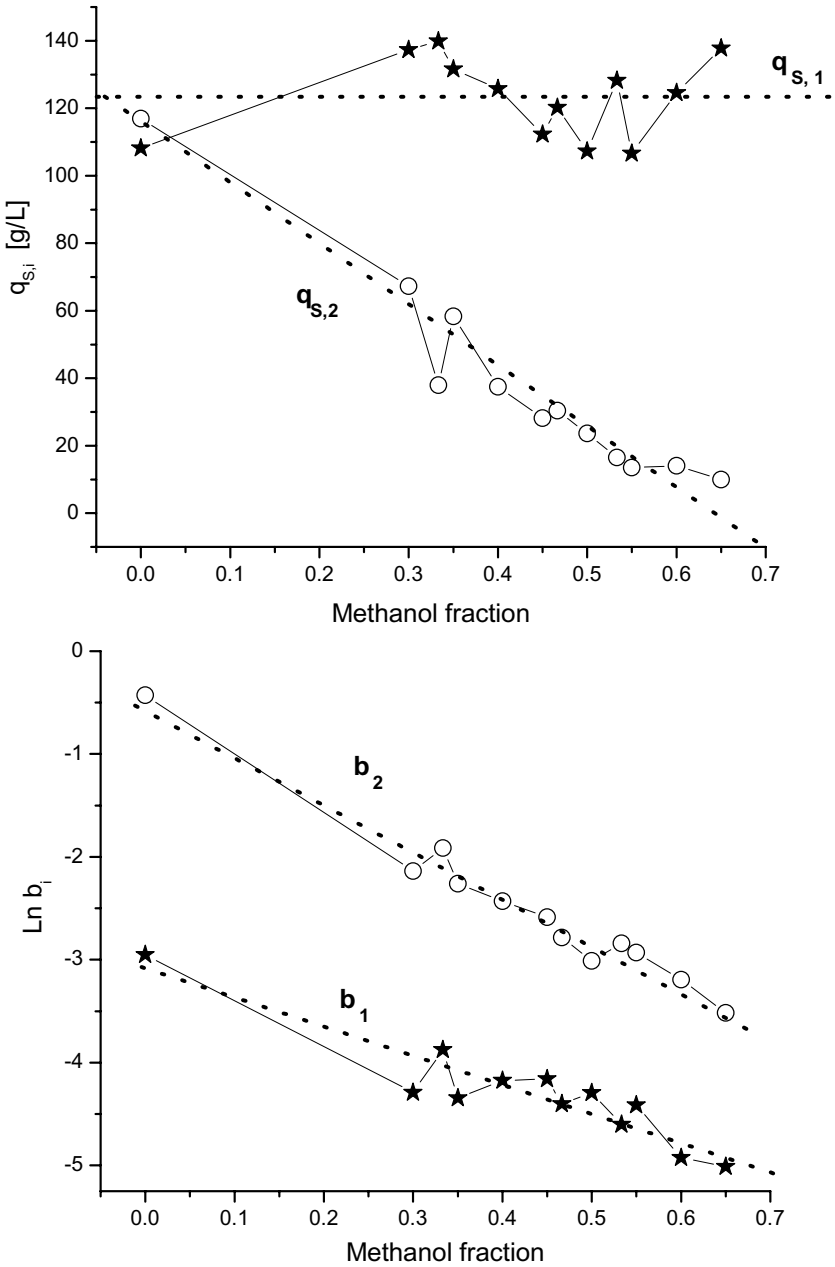

Fig. 1. Influence of the methanol volume fraction φ in an aqueous mobile phase on the saturation capacity and the equilibrium constant of both types of sites which describe the retention of phenol on the Kromasil-C_{18} column (Bilangmuir isotherm) between $\varphi = 0$ and 0.65. The first graph is the plots of the saturation capacities of each type of sites ($i = 1$ low-energy sites; $i = 2$ high-energy sites) vs. the methanol concentration in the mobile phase. Note the constant value of $q_{S,1}$ and the linear decrease of $q_{S,2}$. Plots of the logarithm of the adsorption constant vs. the methanol concentration in the mobile phase. Note the same effect of the methanol fraction on both adsorption constants (solubility effect).

and the length and time increments of the numerical integration are chosen so that the numerical dispersion balances the dispersion effect caused by the apparent diffusion coefficient D_a. In gradient elution chromatography, only the backward$_{t-1}$—backward calculation scheme is preferred for reasons explained elsewhere [1]. Eq. (3) is then discretized as follows:

$$\frac{C_{z,t} - C_{z,t-\Delta t}}{\Delta t} + u\frac{C_{z,t-\Delta t} - C_{z-\Delta z,t-\Delta t}}{\Delta z} + F\frac{q^*_{z,t} - q^*_{z,t-\Delta t}}{\Delta t} = 0 \quad (4)$$

where Δz and Δt are the space and the time increments, respectively. Eq. (4) rearranges into:

$$C_{z,t} + Fq^*_{z,t} = C_{z,t-\Delta t} + Fq^*_{z,t-\Delta t} - u\frac{\Delta t}{\Delta z}(C_{z,t-\Delta t} - C_{z-\Delta z,t-\Delta t}) \quad (5)$$

The algorithm becomes identical to that of the Craig machine when the length increment is $\Delta z = L/n_c$, where n_c is the number of cells in the Craig machine equivalent to the column, that is $n_c = Nk/(k+1)$ [1], and the time increment is $\Delta t = \Delta z/u$. This means that the mobile phase moves exactly by one cell for each time unit, Δt. However, the integration carried out as described above does not provide directly the axial distributions of the mobile and the stationary phase concentrations. Eq. (5) gives only, once the concentration distribution in the column is known in the cell z at the time $t - \Delta t$, the total amount, $C_{z,t} + Fq^*_{z,t}$, present in the cell z at time t. Hence, $C_{z,t}$ and $q^*_{z,t}$ must be calculated individually to continue the iteration process given by Eq. (5). This is numerically done by using the expression of q^* versus C (Eq. (1)).

The local value of the phase ratio F (and consequently that of u, the interstitial velocity) is actually not uniform along the column but it varies as the front ramp of the gradient moves along the column because the local porosity depends on the mobile phase composition. As the variation is small, however, the total porosity will be kept constant in the numerical solutions of the ED model. Later, we discuss the choice of the value of this parameter used in the calculation.

2.2.2. Initial and boundary conditions for the ED model

At $t = 0$, the concentrations of the compound studied (i.e. of the solute and the adsorbate) in the column are uniformly equal to zero, and the stationary phase is in equilibrium with the pure mobile phase containing the initial volume fraction φ_0 of methanol. The boundary conditions used are the classical Danckwerts-type boundary conditions [1,22] at the inlet and outlet of the column. In all the calculations, the inlet profiles are assumed to be rectangular profiles of width t_p The injection is followed by the programming of a linear solvent gradient at $z = 0$, thus:

$$\varphi(t,0) = \begin{cases} 0, & 0 \le t \le t_p \\ \varphi_0 + \dfrac{\Delta\varphi}{t_g}(t - t_p), & t_p \le t \le t_p + t_g \\ \varphi_0 + \Delta\varphi, & t \ge t_p + t_g \end{cases}$$

where φ_0 and $\Delta\varphi$ are the initial methanol fraction and the height of the linear gradient procedure and t_g is the time duration of the gradient. The ramp is assumed to move through the column with the interstitial velocity u. We define β as the slope of the gradient, $\beta = \Delta\varphi/t_g$.

3. Experimental

3.1. Chemicals

The mobile phase used in this work consists in solutions of methanol and water of variable composition. Both solvents were of HPLC grade and purchased from Fisher Scientific (Fair Lawn, NJ, USA). The mobile phase was filtered before use on an surfactant free cellulose acetate filter membrane, 0.2 μm pore size (Suwannee, GA, USA). Thiourea was chosen to measure the column hold-up volume at different methanol contents in the mobile phase. Phenol was used as the sample in this work. Thiourea and phenol were obtained from Aldrich (Milwaukee, WI, USA).

3.2. Materials

A manufacturer-packed, 250 mm × 4.6 mm Kromasil column was used (Eka Nobel, Bohus, Sweden, EU). This column was packed with particles of C_{18}-bonded, endcapped, porous silica. This column (Column #E6022) was one of the lot of 10 columns

Table 2
Physico-chemical properties of the packed Kromasil-C_{18} (Eka) Column #E6022

Particle size	5.98 μm
Particle size distribution (90:10, % ratio)	1.44
Pore size; pore volume	112 Å; 0.88 ml/g
Surface area	314 m^2/g
Na, Al, Fe content (ppm)	11; <10; <10
Particule shape	Spherical
Total carbon	20.0%
Surface coverage	3.59 μmol/m^2
Endcapping	Yes

previously used by Kele and Guiochon [23] and Gritti and Guiochon [24] (Columns E6019, #E6103–E6106, #E6021–E6024 and #E6436 for their study of the reproducibility of the chromatographic properties of RPLC columns under linear and non-linear conditions, respectively. The main characteristics of the bare porous silica and of the packing material used are summarized in Table 2.

The hold-up time of this column was derived from the retention times of two consecutive injections of thiourea at variable methanol contents after the column was let to equilibrate for an hour at a given mobile phase composition. Thiourea is a suitable organic marker for the determination of the hold-up volume, because it gives the same value of the hold-up time as the one determined from the retention times of a few components belonging to the same homologous series. The increase of the elution time of thiourea with decreasing methanol concentration is due to the larger accessible pore volume, not to a significant adsorption of thiourea on the C_{15}-bonded adsorbent [25,26].

3.3. Apparatus

The overloaded band profiles of phenol were acquired using a Hewlett-Packard (now Agilent Technologies, Palo Alto, CA, USA) HP 1090 liquid chromatograph. This instrument was preferred to others available because it has a very small volume between the mixing chamber and the column inlet. This instrument includes a multi-solvent delivery system containing three solvent tanks of volume 1 l each. The tanks were filled, tank A with pure water, tank B with the phenol solution in pure water, and tank C with pure methanol. The instruments includes also an auto-sampler with a 250 μl sample loop, a diode-array UV-detector, a column thermostat and a data station. Compressed nitrogen and helium bottles (National Welders, Charlotte, NC, USA) are connected to the instrument to allow the continuous operation of the pump, the auto-sampler, and the solvent sparging.

The extra-column volumes are 0.058 and 0.93 ml as measured from the auto-sampler and from the pump mixer system, respectively, to the column inlet. All the retention data were corrected for this contribution. The flow-rate accuracy was checked by pumping the pure mobile phase at 23 °C and 1 ml/min during 50 min, from each pump head, successively, into a volumetric glass of 50 ml. The relative error was <0.4%, so that we can estimate the long-term accuracy of the flow-rate at 4 μl/min at flow rates around 1 ml/min. All measurements were carried out at a constant temperature of 23 °C, fixed by the laboratory air-conditioner. The daily variation of the ambient temperature never exceeded ±1 °C.

3.4. Detector calibration

The comparison between experimental and calculated band profiles requires the conversion of the experimental band profiles from the recorded absorbance profiles into concentration profiles. By comparison to the simple isocratic mode of chromatography, an additional complication arises in overloaded gradient elution experiments from the fact that, as soon as the detector response ceases to be linear, the calibration curves depend, at least to some extent, on the concentration of the organic modifier (methanol in this work). This phenomenon must be taken into account, especially at high loading factors, because the chromatographic band width is large enough for the methanol concentration to vary significantly between the beginning and the end of the band. This means that a two-dimension regression is necessary in order to determine the exact concentration profiles.

Fig. 2 illustrates the change in the calibration curve parameters as a function of the methanol fraction in the mobile phase. It makes obvious that, for a given concentration, *C*, the UV-absorbance increases with increasing methanol content. Fig. 3 shows a plot of the difference between the mass expected for the sample (i.e. the mass actually injected) and the mass converted (i.e. the outlet mass recalculated with the

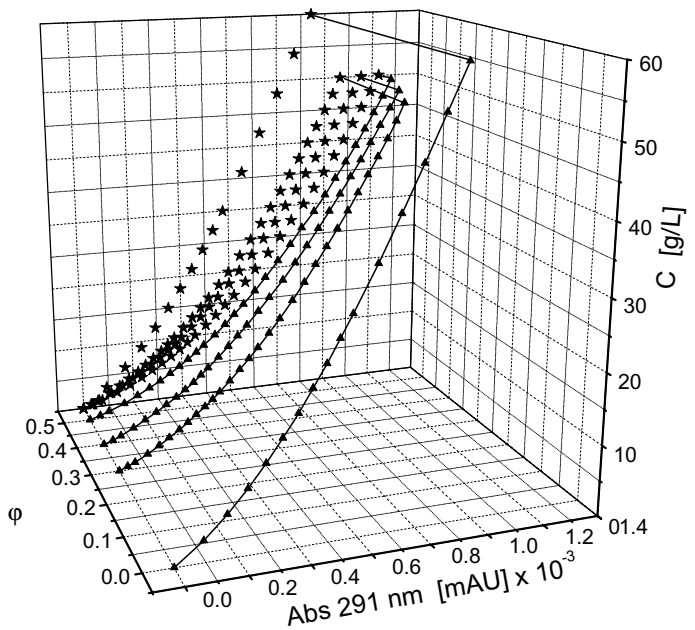

Fig. 2. Three-dimensional representation of the calibration curve (connected full triangles) of phenol dissolved in various mixtures of methanol and water. φ is the volume fraction of methanol ($\varphi = 0$, 0.3, 0.4 and 0.5). Note for a given concentration, the larger absorption in solvents richer in methanol (full stars: projection of the calibration curves on the Abs, C plan).

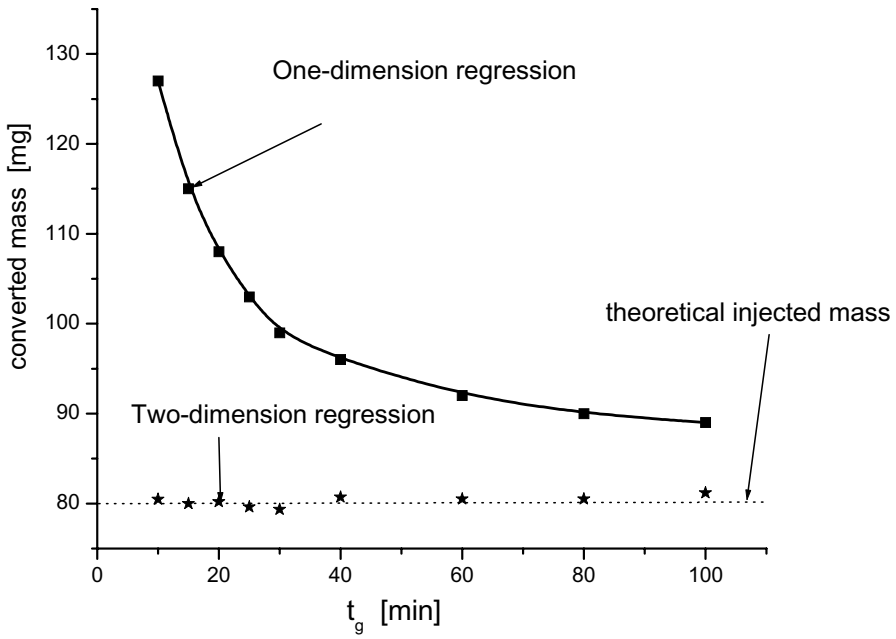

Fig. 3. Recalculation of the column outlet mass using a one-dimension ($C = f$(Abs), connected full squares) and a two-dimension regression calibration curve ($C = f$(Abs,φ), stars plot). The one-dimension curve is that measured in pure water. Note the necessary correction provided by the two-dimensional calibration curve (see text) to predict the actual eluted mass of phenol (40 g/l during 2 min at 1 ml/min or 80 mg).

calibration curves) versus the gradient time t_g in two different cases, the first, when a simple one-dimension regression is used and the second, when the more accurate two-dimension regression is used. In the first case, the one-dimension curve was calculated with pure water $C(\text{Abs}, \varphi = 0)$. Accordingly, the calculated mass is overestimated at high gradient steepness, because the methanol concentration varies significantly from the beginning to the end of the band profile and the absorbance of phenol increases. According to the variation of C versus φ for a few fixed absorbance levels, the two-dimensional regression was well approximated by the following correlation:

$$C(\text{Abs}, \varphi) = [A\text{Abs} + B\text{Abs}^2 + C\text{Abs}^3](1 - 1.03\varphi) \quad (7)$$

In this equation, Abs is the absorbance recorded at 291 nm for a given concentration C of phenol in a mobile phase containing a φ methanol fraction, while A, B and C are the best parameters of the calibration curve measured in pure water. This equation was used to transform all the absorbance profiles of the eluent recorded in overloaded gradient chromatography into concentration profiles, knowing φ as a function of time at the outlet of the column ($z = L$). Since we assumed, in agreement with previous measurements [16], that the strong solvent methanol is not adsorbed on the stationary phase, the gradient ramp is simply translated along the column, propagating with the interstitial velocity u. Then, the methanol fraction in the mobile phase $\varphi(t, L)$ at the outlet of the column is given by:

$$\varphi(t, L) = \varphi_0, \quad 0 \le t \le \frac{L}{u} \quad (8a)$$

$$\varphi(t, L) = 0, \quad \frac{L}{u} \le t \le \frac{L}{u} + t_p \quad (8b)$$

$$\varphi(t, L) = \varphi_0 + \beta\left(t - t_p - \frac{L}{u}\right), \quad \frac{L}{u} + t_p \le t \le \frac{L}{u} + t_p + t_g \quad (8c)$$

$$\varphi(t, L) = \varphi_0 + \Delta\varphi, \quad t \ge \frac{L}{u} + t_p + t_g \quad (8d)$$

where L/u is the hold-up time of the column when equilibrated with the initial methanol content in the mobile phase, φ_0. As a result of this calibration exercise, the mass of phenol eluting from the column, calculated using Eq. (7), is more accurate than if derived from the simple on dimension regression (see Fig. 3) and it agrees very well with the injected mass.

3.5. Overloaded gradient elution profiles

Two series of gradient elution measurements were made. The first one was carried out with a 40 g/l solution of phenol dissolved in pure water. At the beginning of all these gradient programs, the column was equilibrated with pure water. The methanol fraction, φ, was increased linearly, at a rate between 0.5 and 5%/min, with nine different gradient times t_g equal to 10, 15, 20, 25, 30, 40, 60, 80, and 100 min. The second series of measurements was carried out with a solution of 15 g/l of phenol dissolved in pure water. At the beginning of all these gradient elutions, the column was equilibrated with a solution of methanol and water at $\varphi = 0.05$. Various gradient heights were performed ($\Delta\varphi = 0.1$, 0.2, 0.3 and 0.4) within two different time durations ($t_g = 25$ min for $\Delta\varphi = 0.4$ and $t_g = 50$ min for $\Delta\varphi = 0.1$, 0.2 and 0.3).

4. Results and discussion

4.1. Importance of the local porosities of the C_{18}-bonded column in gradient elution chromatography

Conventional numerical calculations of overloaded band profiles assume that the column porosity is constant [1,3]. This is not necessarily true in gradient elution because the internal porosity of the particles depends usually on the organic modifier content, which varies along the column during the elution of the band profile. The porosity distribution along the column depends on the slope of the gradient. So, the local porosity ε_t at the distance z along the column is actually not constant but varies with time. So, does the phase ratio F.

The true column porosity was derived from measurements of the column hold-up volume as a function of the methanol concentration in the mobile phase. The methanol volume fraction was decreased stepwise ($\Delta\varphi = -0.05$) from 0.5 to 0. For each step, the retention time of thiourea was measured twice. The results are reported in Fig. 4. They show a significant increase of the local porosity, due to the folding and/or

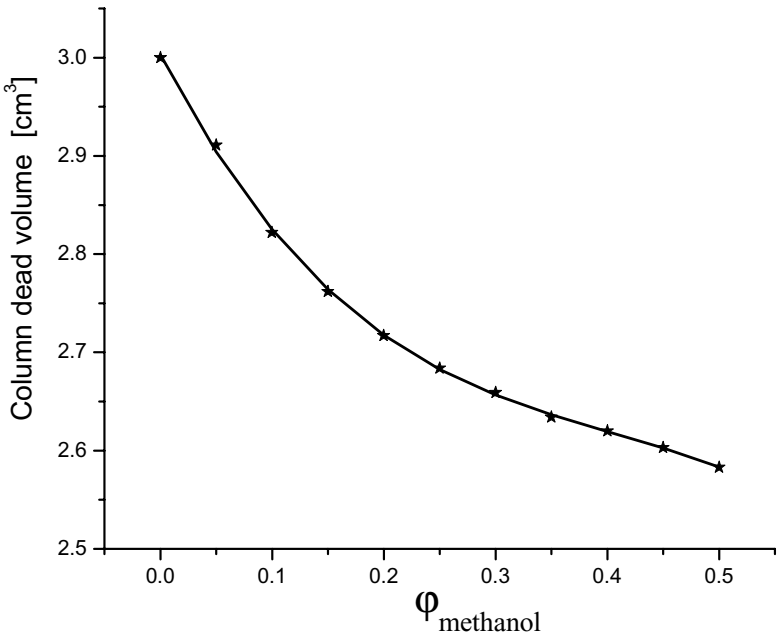

Fig. 4. Dead volume of the Kromasil-C_{18} column (250 mm × 4.6 mm) measured by thiourea injections as a function of the methanol fraction in the mobile phase from $\varphi = 0.5$ to 0.

collapsing of the C_{18} chains when the methanol concentration of the mobile phase decreases. The experimental total porosity was fitted to a third order polynomial, as follows:

$$\varepsilon(\varphi) = \varepsilon(0) + a\varphi + b\varphi^2 + c\varphi^3 \quad (9)$$

The non-linear regression of the experimental data to this model gave as best estimates for the parameters *ε(0)*, *a*, *b* and *c* the values 0.722, −0.530, 1.116 and −0.921, respectively. Eq. (9) was used to determine the best physically acceptable value of the constant and time average column porosity, ε_{exp} required for the numerical calculation of band profiles in gradient elution. Two definitions of ε_{exp} were used.

First, it was assumed that the column porosity was equal to the arithmetic average of the initial column porosity, just before the sample injection, and the porosity at the time, t_{shock}, when the front shock is eluted. This gives:

$$\varepsilon_{exp,1} = \frac{\varepsilon(0, L) + \varepsilon(t_{shock}, L)}{2} \quad (10)$$

This first estimate lacks physical meaning because it does not follow the migration of the front shock along the column.

A second estimate of the column porosity was made, based on the realization that the ED program calculates the band profile along the column at successive times $t_j = j\Delta t$ (j is an integer). The local column porosity was calculated in the simulation program by using Eq. (9), at the location of the shock in the column ($0 \leq z_{shock} \leq L$) at each time t_j between the beginning of the injection ($t = 0$) and the outlet detection of the shock ($t = t_{shock}$). For each time increment in the calculation, the position of the maximum of the band profile was taken as the position of the shock. $\varepsilon_{exp,2}$ resulted in the arithmetic average of all these porosities. Whatever the constant porosity required in the simulation, the result converged toward the same and unique value. The $\varepsilon_{exp,2}$ should mirror better the actual average column porosity at the shock location than $\varepsilon_{exp,1}$ does.

$$\varepsilon_{exp,2} = \frac{1}{N}\sum_{i=1}^{i=N} \varepsilon_{shock}(i) \quad (11)$$

where $N = t_{shock}/\Delta t$.

The relative value of these two choices of handling the variations of the column porosity during gradient elution is discussed later, with the comparison between

calculated and experimental band profiles and, more specifically, the position of the front shocks.

4.2. Retention time in gradient elution under linear conditions

The fundamental equation for retention in gradient elution is [7,9]:

$$\int_0^{V_S} \frac{dV}{V_a} = 1 \tag{12}$$

where V_S is the corrected retention volume of the band center, with $V_S = V_R - V_0$, where V_R is the retention volume, V_0 the volume of mobile phase initially present in the column, that always precedes the band center. dV refers to a differential volume of mobile phase that passes through the band center during its migration along the column, and $V_a = V_a(t)$ is the instantaneous or "actual" value of the corrected retention volume at any given time. Let $k_a = k_a(t)$ be the instantaneous value of k for the band (function of φ at the band center), then

$$V_a = k_a V_0 \tag{13}$$

Eq. (12) can be simply rewritten with time as the variable, since the flow rate, F_v, is constant during elution ($V = F_v t$). Then

$$\int_0^{t_S} \frac{dt}{k_a} = t_0 \tag{14}$$

Note that, in this equation, the hold-up time of the column, t_0, is assumed to be constant, independent of the gradient parameters, which is an approximation. The instantaneous retention factor k_a is derived from the initial slope of the general isotherm equation (Eq. (1), where the concentration C tends toward 0) and from the constant phase ratio F. k_a depends on φ, which is a function of time t:

$$\frac{k_a}{F} = (q_{2,0} - S_{q_2}\varphi_0 - S_{q_2}\beta t) b_{2,0} \exp(-S_{b_2}\varphi_0) \exp(-S_{b_2}\beta t) + q_{1,0}\, b_{1,0} \exp(-S_{b_1}\varphi_0) \exp(-S_{b_1}\beta t) \tag{15}$$

There are no algebraic solutions for a combination of Eqs. (13) and (14) and t_S can only be determined

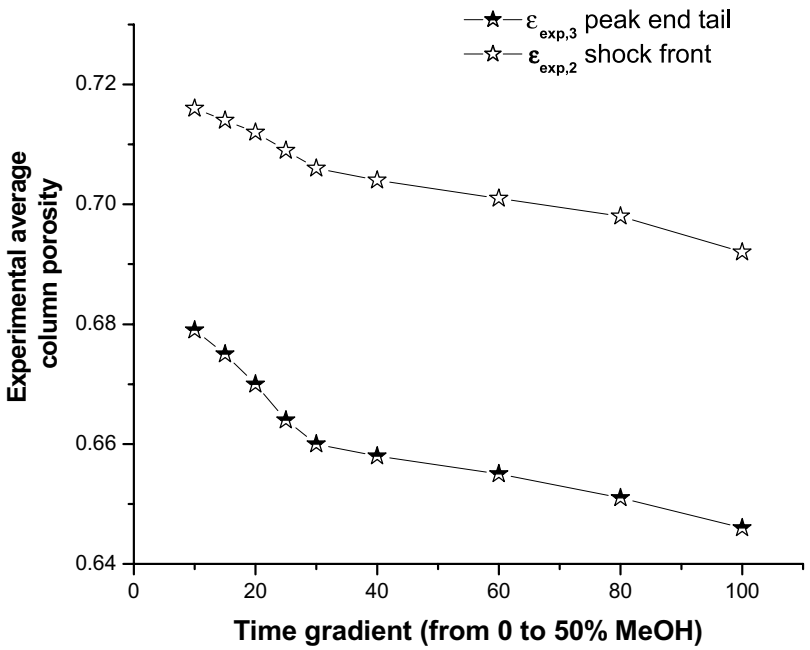

Fig. 5. Plots of the convergent average porosities $\varepsilon_{exp,2}$ (located at the shock position) and $\varepsilon_{exp,3}$ (located at the peak end tail) calculated during the simulation from the experimental data fitted in Fig. 4 (see text) vs. the gradient time required to jump from 0 to 50% methanol in the mobile phase.

numerically. Since actually t_0 is not constant, it will also be derived from independent experimental porosity data. Obviously, this porosity estimate should be different from $\varepsilon_{exp,1}$ or $\varepsilon_{exp,2}$ because (with a Bilangmuir isotherm) the low concentrations of a band move under linear or quasi-linear conditions, are more retained than the high concentrations, and spend a longer time inside the column. A third empirical average porosity $\varepsilon_{exp,3}$ was defined as the average of the local porosities along the trajectory of the maximum concentration of a band migrating at the limit velocity of the concentration $C = 0$, i.e. at the velocity of the center of an analytical band (retention time, $t = t_{R,0}$).

$$\varepsilon_{exp,3} = \frac{1}{N'} \sum_{j=1}^{j=N'} \varepsilon_{R,0}(j) \tag{16}$$

where $N' = t_{R,0}/\Delta t$.

Fig. 5 compares the two calculated porosities, $\varepsilon_{exp,2}$ and $\varepsilon_{exp,3}$ The latter is markedly smaller than the former since: (1) the column porosity decreases with increasing methanol content; (2) the average methanol content of the column increases with increasing time; and (3) high phenol concentrations migrate faster than low concentrations. Fig. 6 demonstrates the validity of the variation of the Henry constant with the methanol fraction given by Eq. (15). The band profiles calculated for an analytical injection match very well with the tail end of all the overloaded bands (only the case corresponding to a gradient time of 40 min is shown). For the sake of consistency, each experimental overloaded peak should be corrected by the time width t_p of the injection band (i.e. 2 min). The correct predicted retention time $t_{R,pred}$ is exactly:

$$t_{R,pred} = t_{R,sim} - \frac{V_C}{F_v}(\varepsilon_{exp,3} - \varepsilon(0)) \tag{17}$$

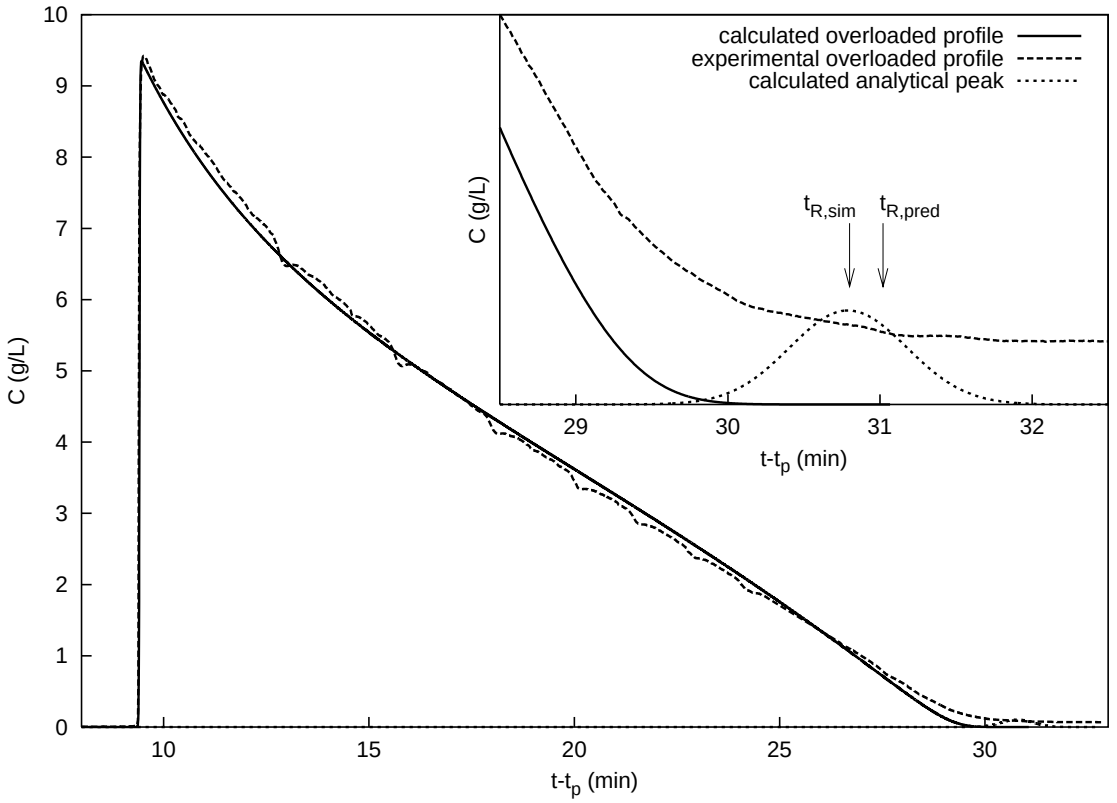

Fig. 6. Comparison between the calculated analytical peak and the experimental end tail profile corrected by the injection time t_p.

where the second term of the RHS takes into account the fact that the column is initially filled and equilibrated with pure water, for which the column porosity is $\varepsilon(0)$, not $\varepsilon_{exp,3}$ as used in the calculation of the profile obtained for an analytical injection. V_C is the column tube volume. For all analytical injections, this correction is smaller than 1% of the retention time (see Fig. 6). Note also that the tail of the overloaded profile calculated with the best value of the porosity for the migration of high-concentrations (the one that gives calculated front shocks matching well experimental ones) is eluted earlier because $\varepsilon_{exp,2}$ is an erroneous estimate of the total porosity for the migration of analytical concentrations. It is markedly larger than $\varepsilon_{exp,3}$, i.e. 0.721 instead of 0.658. The experimental overloaded band profile extends well beyond the time predicted probably because of the slow mass transfer kinetics that probably takes place at very low methanol concentration.

Since the complete model of retention in gradient elution chromatography has been validated under linear conditions, it can be applied now to chromatography under non-linear conditions.

4.3. Comparison between experimental and simulated overloaded profiles

In the first series of experiments, the amplitude of the change of the concentration of methanol at the end of the gradient was kept constant. This concentration increased linearly from 0 to 50% during different gradient times (10, 15, 20, 25, 30, 40, 60, 80 and 100 min). Accordingly, the rate of variation of the relative concentration of methanol in the mobile phase varies between 0.5 and 5%/min. The injection of the same amount of phenol (a 40 g/l solution of phenol in pure water during 2 min) was performed in the nine experiments. All profiles were calculated using different values of the porosity and the one that gives the best match between the experimental and the calculated front shock was selected as the best empirical value of the porosity. Fig. 7 shows the excellent agreement between these empirical estimates of the porosity and those suggested earlier. There is a strong correlation between these empirical values on the one hand and $\varepsilon_{exp,1}$ and $\varepsilon_{exp,2}$ defined in Section 4.1, earlier, and directly derived from the dependence of the porosity on

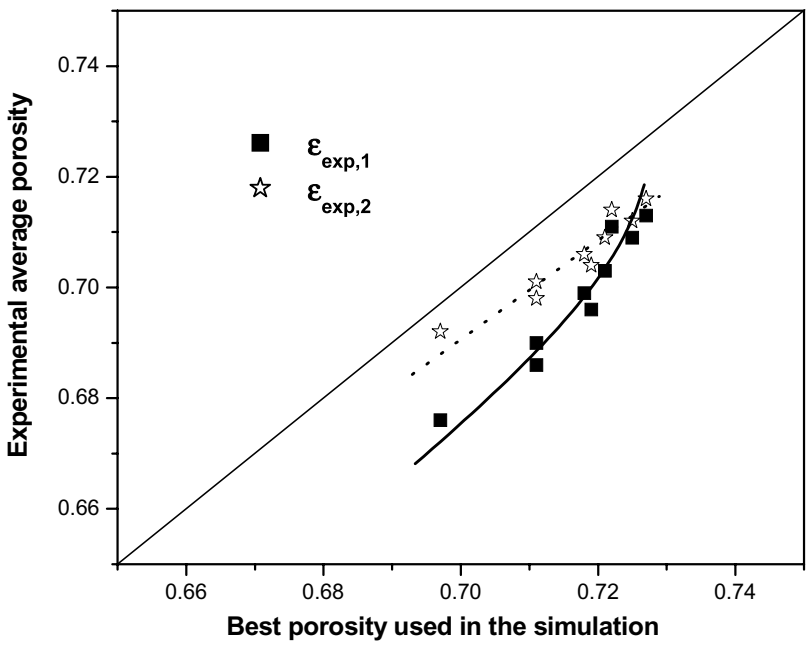

Fig. 7. Comparison between the best porosities arbitrary chosen in the simulation of overloaded profiles and those determined independently, $\varepsilon_{exp,2}$ and $\varepsilon_{exp,1}$ plotted in Fig. 5. Note the very good agreement between $\varepsilon_{exp,2}$ and the simulated porosity with a shift of only −0.01 (≤1.5%).

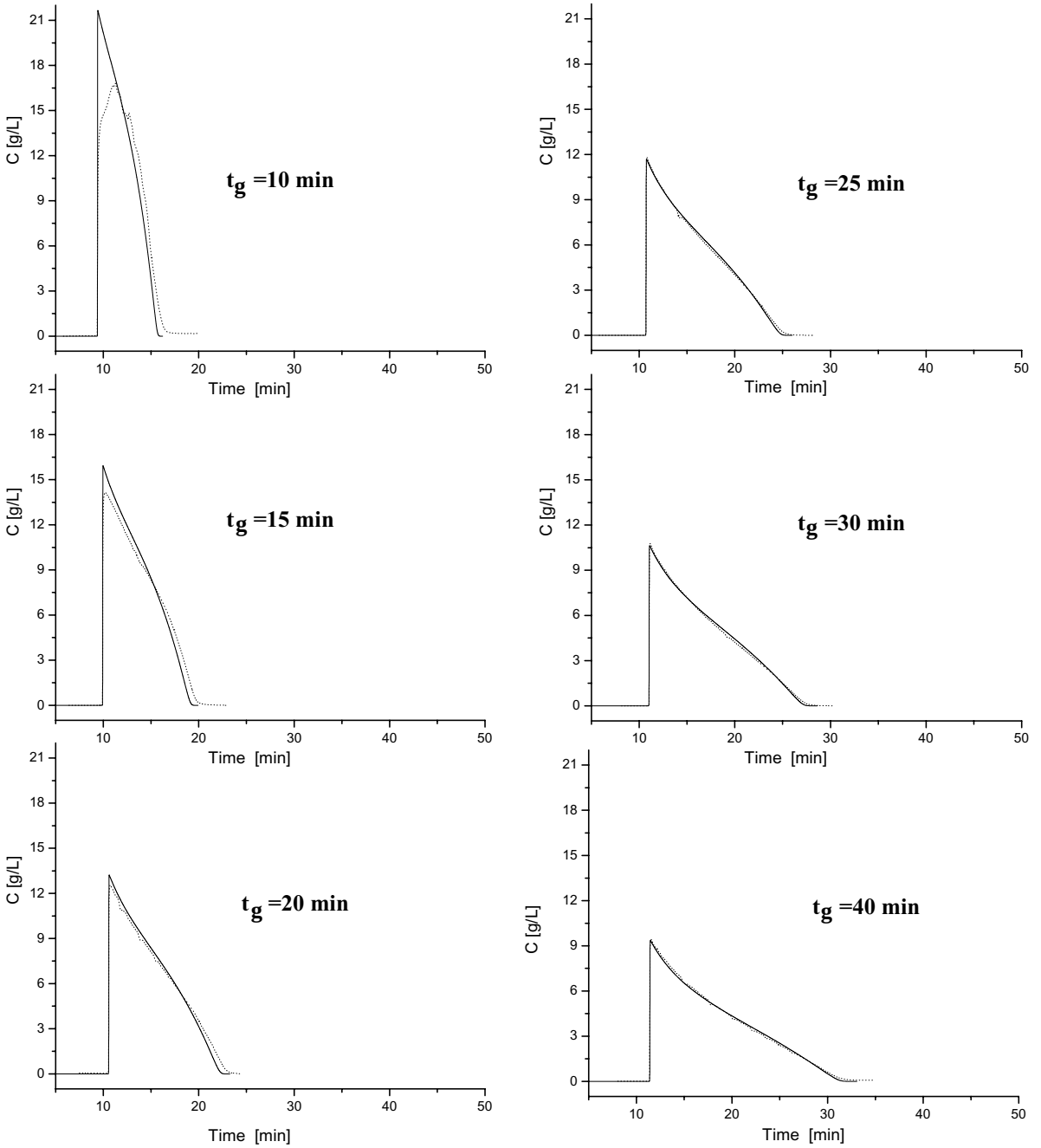

Fig. 8. Comparison between the experimental (dotted lines) and calculated band profiles (solid lines) for nine different gradient times t_g at high column loading (80 mg injected). Injection of a 40 g/l solution of phenol dissolved in pure water during 2 min. Flow rate, 1 ml/min; gradient step, 0–50% methanol.

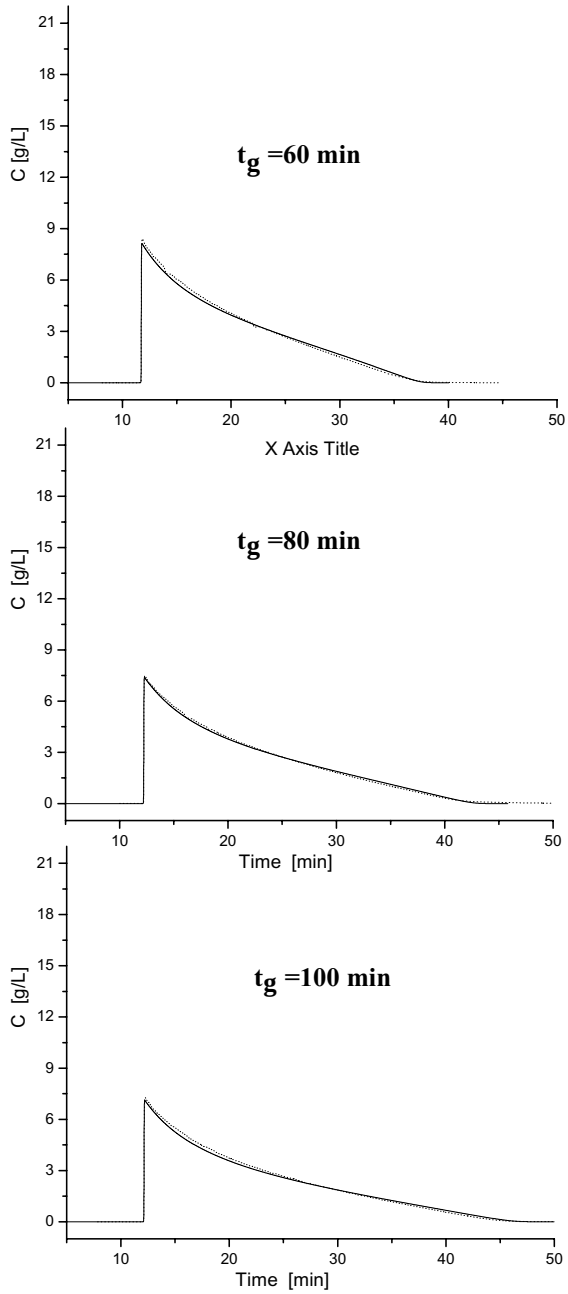

Fig. 8. (*Continued*).

the methanol concentration. As expected, $\varepsilon_{exp,2}$ is a more accurate estimate than $\varepsilon_{exp,1}$, especially at high gradient steepness, for which the porosity is the lowest. However, there is still a small but significant and systematic difference of approximately 0.01, i.e. 1.5% between $\varepsilon_{exp,2}$ and the best average porosity. This exercise demonstrates that the best choice of the constant porosity used in the calculations is consistent with the actual variation of the porosity inside the column. The ideal situation would be to calculate the overloaded band profiles by using a variable local porosity, $\varepsilon_{z,t}$, in the mass balance equation of the ED model. Then, however, Eq. (3) is no longer valid and the numerical solution used here (Eqs. (4) and (5)) must be reconsidered. Our results show that it is not necessary to do so in order to achieve satisfactory predictions of band profiles.

The agreement between the experimental and calculated rear part of the band profiles is always excellent (Fig. 8). There are significant differences between the top part of these profiles only when β is larger than 3% methanol/min. This disagreement may possibly stem from a slow rate of equilibration between the stationary and the mobile phases in contact. The chromatographic system remains at equilibrium only if the kinetics of the C_{18} chains rearrangement is sufficiently fast to "follow" the variation of the mobile phase composition in the interfacial region. This effect explains probably the obvious differences observed between calculated and experimental profiles for the two steepest gradients (3.33 and 5.0%). Similar deviations were observed by El Fallah and Guiochon [10,11] at very steep gradients for the elution profiles of 2-phenyethanol with acetonitrile as the organic modifier. They found good agreement between calculated and experimental profiles for shallow and moderate gradient steepness (1 or 2% ACN/min) but strong discrepancies appeared at 4% ACN/min. The kinetics of wetting of a solid surface by a liquid phase and that of the reorganization of the bonded chains in a liquid of changing compositions are still not sufficiently well understood. We recently showed [16] that the slow rate at which the bonded alkyl chains that were collapsed in pure water dissolve into the organic solution during frontal analysis controls the shape of the breakthrough curves. This phenomenon makes difficult the accurate modeling of band profiles under steep gradient conditions. The simple equilibrium-dispersive model of chromatography cannot describe accurately their shapes. The proper kinetic equations should be introduced in the general model but the kinetics of the chain dissolution should first be unraveled.

In the second series of measurements performed in this work, the initial concentration of methanol in the mobile phase was low but finite, the column being first equilibrated with a 5% methanol mobile phase. The loading factor was divided by a factor of about 5 compared to the previous series of experiments, by injecting a 15 g/l solution of phenol in pure water, during only 1 min. The methanol content was increased

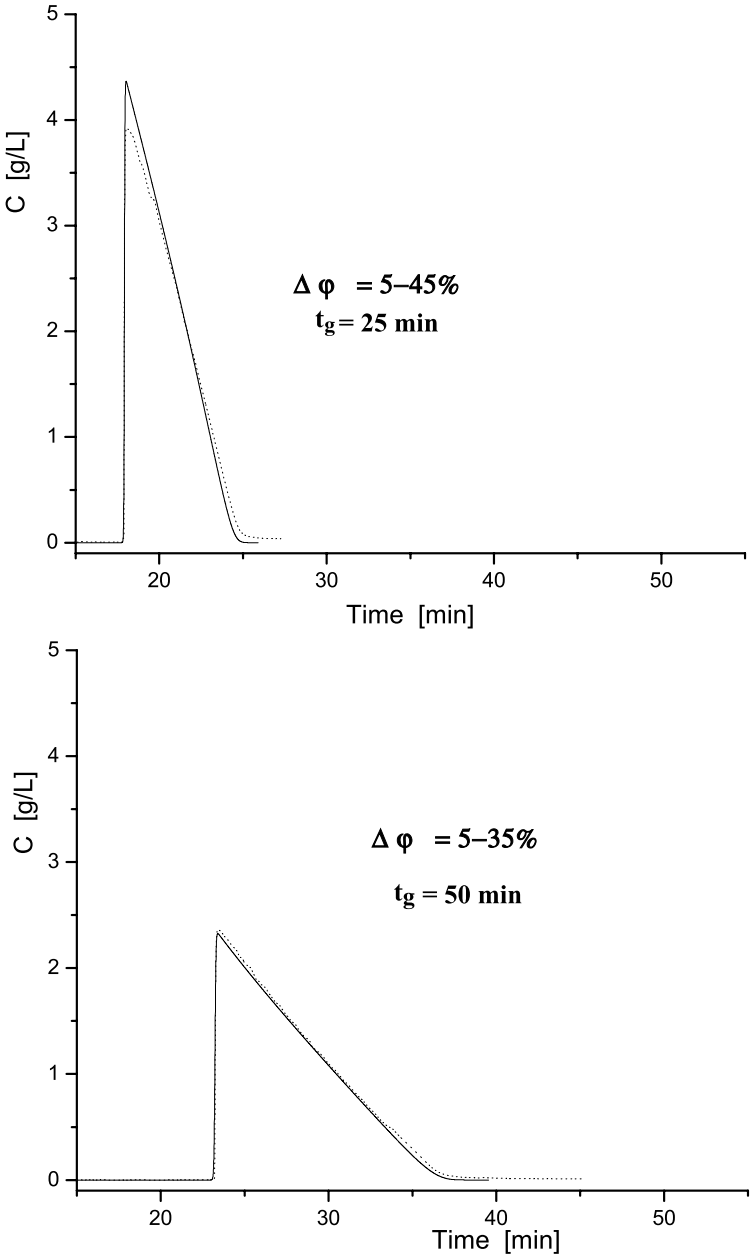

Fig. 9. Comparison between experimental and calculated band profiles at low column loading (15 mg injected). Injection of a 15 g/l solution of phenol dissolved in pure water during 1 min. Flow rate, 1 ml/min.

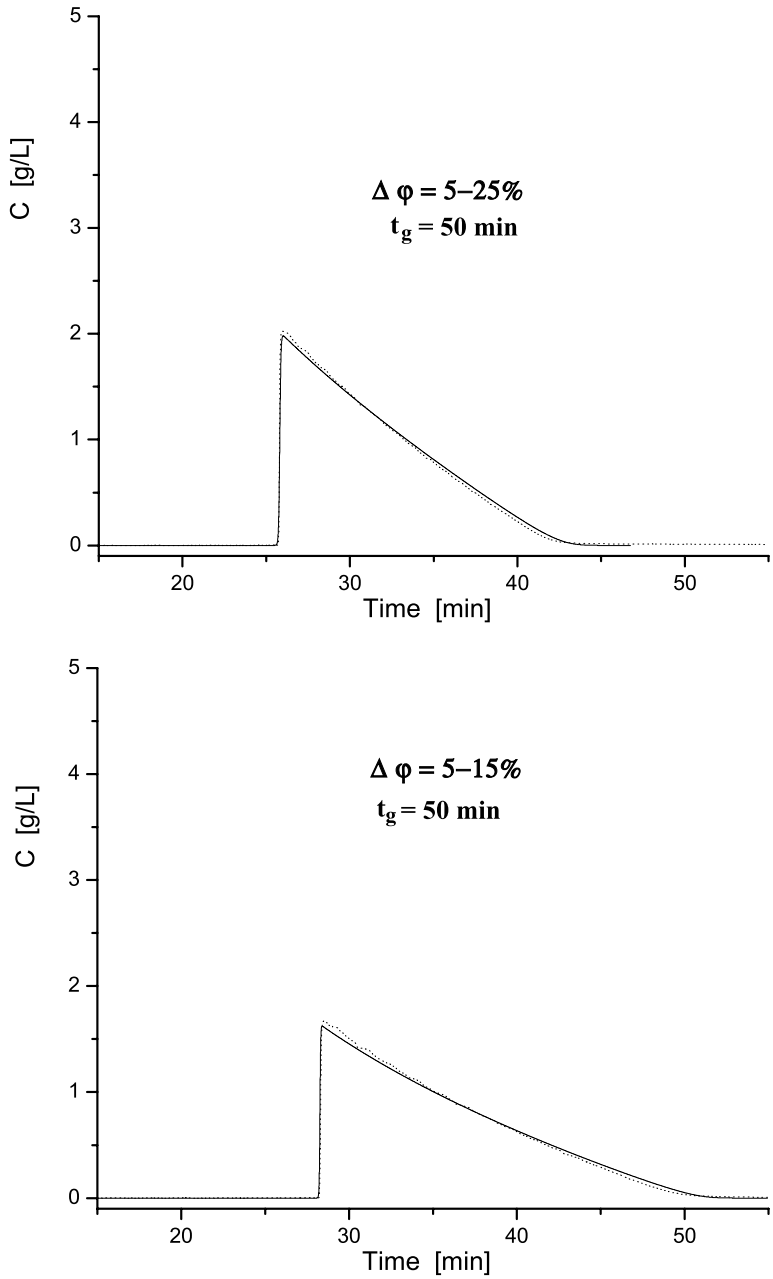

Fig. 9. (*Continued*).

from 5 to 45, 35, 25 and 15% with gradient times of 25 min in the former case and 50 min in the other three experiments. Hence, the values of β were relatively low, at 1.6, 0.6, 0.4 and 0.2% MeOH/min, respectively. Under these different experimental conditions, a very good agreement between experimental and calculated profiles is observed (Fig. 9). This is so mostly because β is small, well below 3% MeOH/min and the mobile and stationary phases remain constantly in equilibrium.

5. Conclusion

Our results confirm that the adsorption behavior of phenol onto a C_{18}-bonded silica column, from methanol–water solutions, is well described by an original general Bilangmuir isotherm model. This adsorption isotherm is more complex than those used previously, it accounts well for the strong variations of the saturation capacity of the surface with the methanol concentration, and it permits an accurate prediction of the profiles of low and high concentration bands in gradient elution, even with relatively steep gradients, up to 3% methanol/min, and even when the initial mobile phase is pure water. Significant discrepancies are observed with still steeper gradients, as already observed in prior work [10,11]. The finite rate of the rearrangement of the C_{18} chains in contact with a mobile phase of rapidly changing composition explains these discrepancies. The need for the alkyl chains bonded to the silica surface to undergo strong conformation changes at very low methanol concentrations represents a limit in the modeling of overloaded band profiles in liquid chromatography. Not only the knowledge of the mass transfer kinetics of the solute between the stationary and the mobile phases is necessary, but also the knowledge of the rate of rearrangement of the interfacial region is required in order to accurately model band profiles at high water concentrations.

Acknowledgements

This work was supported in part by Grant CHE-00-70548 of the National Science Foundation and by the cooperative agreement between the University of Tennessee and the Oak Ridge National Laboratory. We thank Hans Liliedahi and Lars Torstenson (Eka Nobel, Bohus, Sweden) (and the other people for the other column) for the generous gift of the columns used in this work and for fruitful discussions.

References

[1] G. Guiochon, S.G. Shirazi, A.M. Katti, Fundamentals of Preparative and Non-linear Chromatography, Academic Press, Boston, MA, 1994.
[2] G. Gujochon, J. Chromatogr. A 965 (2002) 129.
[3] B. Lin, G. Gujochon, Modeling for Preparative Chromatography, Elsevier, Amsterdam, The Netherlands, 2003.
[4] J.H. Knox, M. Pyper, J. Chromatogr. 363 (1986) 1.
[5] A. Felinger, G. Guiochon, J. Chromatogr. 591 (1992) 31.
[6] A. Fehnger, G. Guiochon, J. Chromatogr. 609 (1992) 35.
[7] L.R. Snyder, High Performance Liquid Chromatography—Advances and Perspectives, Elsevier, Amsterdam, The Netherlands, 1985.
[8] F.D. Antia, Cs. Horváth, J. Chromatogr. 484 (1989) 1.
[9] P. Jandera, J. Churácek, Gradient Elution in Column Liquid Chromatography: Theory and Practice, Elsevier, Amsterdam, The Netherlands, 1985.
[10] M.Z. El Fallah, G. Gujochon, Anal. Chem. 63 (1991) 859.
[11] M.Z. El Fallah, G. Guiochon, Anal. Chem. 63 (1991) 2244.
[12] M.Z. El Fallah, G. Gujochon, Biotechnol. Bioeng. 39 (1992) 877.
[13] A. Felinger, G. Guiochon, Biotechnol. Bioeng. 12 (1996) 638.
[14] A. Felinger, G. Guiochon, J. Chromatogr. A 796 (1998) 59.
[15] F. Gritti, G. Gujochon, J. Chromatogr. A 1010 (2003) 153.
[16] F. Gritti, G. Guiochon, J. Chromatogr. A 995 (2003) 37.
[17] F. Gritti, G. Guiochon, submitted for publication.
[18] D. Graham, J. Phys. Chem. 57 (1953) 665.
[19] D.M. Ruthven, Principles of Adsorption and Adsorption Process, Wiley, New York, 1984.
[20] M. Suzuki, Adsorption Engineering, Elsevier, Amsterdam, The Netherlands, 1990.
[21] P. Rouchon, M. Schonauer, P. Valentin, G. Guiochon, Sep. Sci. Technol. 22 (1987) 1793.
[22] P.W. Danckwerts, Chem. Eng. Sci. 2 (1953) 1.
[23] M. Kele, G. Guiochon, J. Chromatogr. A 855 (1999) 423.
[24] F. Gritti, G. Guiochon, J. Chromatogr. A 1003 (2003) 73.
[25] C.R. Yonker, T.A. Zwier, M.F. Burke, J. Chromatogr. 241 (1982) 257.
[26] C.R. Yonker, T.A. Zwier, M.F. Burke, J. Chromatogr. 241 (1982) 269.